

Original Article

Water extract of Galla Rhois with steaming process enhances apoptotic cell death in human colon cancer cellsNam-Hui Yim, Min Jung Gu, Youn-Hwan Hwang, Won-Kyung Cho^{*,☆}, Jin Yeul Ma^{*,☆}

Korean Medicine (KM) Application Center, Korea Institute of Oriental Medicine (KIOM), Daegu, Korea

ARTICLE INFO

Article history:

Received 23 August 2016

Received in revised form

28 September 2016

Accepted 3 October 2016

Available online 11 October 2016

Keywords:

ellagic acid

Galla Rhois

gallic acid

human colon cancer cells

steaming process

ABSTRACT

Background: Galla Rhois has been considered to have medicinal properties against diarrhea, excessive sweating, bleeding, and chronic cough in Asian countries. Gallotannins, which are Galla Rhois-derived tannins, have been reported to possess biological and pharmacological activities, especially anticancer activity. In this study, we evaluated the effect of steaming at a temperature over 120 °C on the chemical constituents and biological activities of the water extract of Galla Rhois (GRE).

Methods: GRE was steamed at a temperature over 120 °C (AGRE), and its specific constituents were analyzed; the results were validated using a high-performance liquid chromatography–diode array detector system. To evaluate the anticancer effect of GRE and AGRE, cell viability assay, cell cycle analysis, and Western blot analysis were performed in HCT116 human colon cancer cells.

Results: Steaming markedly increased the contents of gallic acid and ellagic acid in GRE, and GRE or AGRE treatment reduced the viability of HCT116 cells. Notably, the steaming process enhanced the growth inhibitory effect of GRE in cancer cells. AGRE induced apoptosis through the activation of caspase-3, caspase-8, and caspase-9. Additionally, AGRE regulated the activation of mitogen-activated protein kinases including extracellular signal-regulated kinase, p38, and c-Jun NH₂-terminal kinase, whereas GRE did not. However, both GRE and AGRE inhibited the activation of AKT.

Conclusion: Compared with GRE, AGRE is more potent in its ability to induce apoptosis in HCT116 cells; therefore, we suggest that the steaming process may be useful as a feasible method for improving the anticancer effect of GRE.

© 2016 Korea Institute of Oriental Medicine. Published by Elsevier. This is an open access article under the CC BY-NC-ND license (<http://creativecommons.org/licenses/by-nc-nd/4.0/>).

* Corresponding authors. Korean Medicine (KM) Application Center, Korea Institute of Oriental Medicine (KIOM), 70 Cheomdan-ro, Daegu 701-300, Korea.

E-mail addresses: wkcho@kiom.re.kr (W.-K. Cho), jyma@kiom.re.kr (J.Y. Ma).

☆ Both authors contributed equally to this work.

<http://dx.doi.org/10.1016/j.imr.2016.10.001>

pISSN 2213-4220 eISSN 2213-4239/© 2016 Korea Institute of Oriental Medicine. Published by Elsevier. This is an open access article under the CC BY-NC-ND license (<http://creativecommons.org/licenses/by-nc-nd/4.0/>).

1. Introduction

In oriental medicine, various processing methods have been applied to herbal medicines in order to improve their therapeutic effects in clinical trials. The processing methods for herbal medicines (such as toasting, steaming, boiling in honey, and dipping or soaking in water, alcohol, or vinegar) can enhance their desirable effect, and reduce side effects and toxicity.¹ Studies investigating changes in chemical constituents and biological activities upon processing have been carried out for several herbal medicines, including *Rei Rhizoma*, *Glycyrrhizae Radix*, *Gardeniae Fructus*, *Zingiberis Siccata Rhizoma*, *Lacca Sinica Exsiccata*, *Machili Cortex*, and *Rehmanniae Radix*.²⁻⁷ In this respect, we applied the steaming process to the water extract of *Galla Rhois* (GRE) at a temperature over 120 °C (AGRE) and identified the associated changes in its chemical constituents and biological efficacy.

Galla Rhois (GR), the gall produced by the aphid *Schlechtendalia chinensis* (Bell), on the leaves of *Rhus chinensis*, has been used as a traditional medicine for treating diarrhea, excessive sweating, bleeding, and chronic coughs in Korea, China, and Japan.^{8,9} Recent studies have reported the biological and pharmacological properties of GR, including antibacterial, anticariogenic, antioxidant, anticancer, antidiabetic, antidiarrheal, anti-inflammatory, and hepatoprotective activities.¹⁰ Furthermore, a phytochemical study on GR reported the characterization of gallotannin, which consists of gallic acid units.^{11,12} Bioactive gallotannins isolated from GR, including pentagalloyl glucose, 3- and 4-galloyl-gallic acid, and 1,2,3,4,6-penta-O-galloyl- β -D-glucoside (PGG), possess numerous medicinal activities and health benefits, particularly anticancer activities.¹³⁻¹⁵

In the present study, we evaluated the change in GR-derived tannins upon applying a steaming method to GRE using high-performance liquid chromatography (HPLC), which showed that the steaming process markedly enhances cell death, especially in colon cancer cells, by increasing the apoptotic properties of GRE.

2. Methods

2.1. HPLC analysis

2.1.1. Chemicals and reagents

The standard compound of gallic acid was purchased from TCI (Tokyo, Japan), and methyl gallate, syringic acid, and penta-O-galloyl- β -D-glucoside were purchased from Sigma-Aldrich (St. Louis, MO, USA). The purity of marker compound determined using HPLC was higher than 98%. HPLC-grade solutions including water and acetonitrile were purchased from J.T. Baker (Austin, TX, USA), and trifluoroacetic acid was purchased from Sigma-Aldrich.

2.1.2. Preparation of standard solution, and herb materials GRE and AGRE

Standard solutions, including gallic acid, methyl gallate, digallic acid, syringic acid, ellagic acid, and PGG, were prepared by dissolving each marker component in pure methanol at

1 mg/mL (Fig. 1A). These stock solutions were stored at -4 °C before analysis. Each stock solution was diluted to an appropriate concentration range for the preparation of calibration curves. GR was purchased from the Korea Medicine Herbs Association (Yeongcheon, Korea) and identified by Professor KiHwan Bae, Chungnam National University, Korea. GRE was prepared using GR with water boiling for 3 hours, as described in a previous study.¹⁶ To prepare the AGRE, GRE was steamed by autoclave (Jeio Tech Co., Daejeon, Korea) treatment (120 °C, 20 minutes) and prepared in the form of powder by freeze drying. For HPLC analysis, 1 mg of GRE or AGRE powder was dissolved in 1 mL of distilled water, passed through a 0.22 μ m filter, and stored at -20 °C before use.

2.1.3. HPLC-diode array UV/VIS detector analysis conditions

The experiments in this study were performed using the Hitachi HPLC system (Hitachi, Tokyo, Japan), obtained using the L-2130 pump, L-2200 auto-sampler, L-2300 column oven, and L-2455 diode array UV/VIS (ultraviolet/visible) detector. The data processor used EZchrom Elite software for Hitachi. The chromatographic column that was used in this experiment was commercially available and was obtained from Optimapak (C₁₈, 4.6 × 250 mm², 5 μ m). The column oven temperature was kept at 30 °C. The mobile phase consisted of water containing 0.2% trifluoroacetic acid (A) and acetonitrile containing 0.2% trifluoroacetic acid (B). The line program was well optimized and conducted as follow: 5% B at 0–20 minutes; 20–45% B at 20–45 minutes; 45–90% B at 45–90 minutes at a flow rate of 1.0 mL/min. The UV spectrum was recorded at 270 nm, and the injection volume was set at 10 μ L. Components were identified via comparison of their retention times with those of authentic standards under identical analysis conditions and UV spectra with an in-house PDA (patron-driven acquisition) library.

2.1.4. Validation of the analytical method

The method was validated for linearity, precision and accuracy. Validation was executed according to the International Conference on Harmonization guidelines.¹⁷

2.1.5. Linearity, limits of detection, and limits of quantification

In order to obtain the calibration curves, working solutions of six different concentrations of each marker compound were prepared from the stock solutions by diluting with 60% methanol. Solutions of six different concentrations were analyzed in three consecutive injections. Calibration curves were constructed by plotting the value of the peak versus the concentration of each analyte. Limits of detection and limits of quantification for each analyte were determined on the basis of the signal-to-noise ratios of 3 and 10, respectively.

2.1.6. Precision and accuracy

Precision of the analytical method was evaluated by intra- and interday tests. The mixture standard solutions of three different concentrations were analyzed. The interday test was performed by analyzing the same standard solution in five replicates each day on 3 consecutive days. The intraday

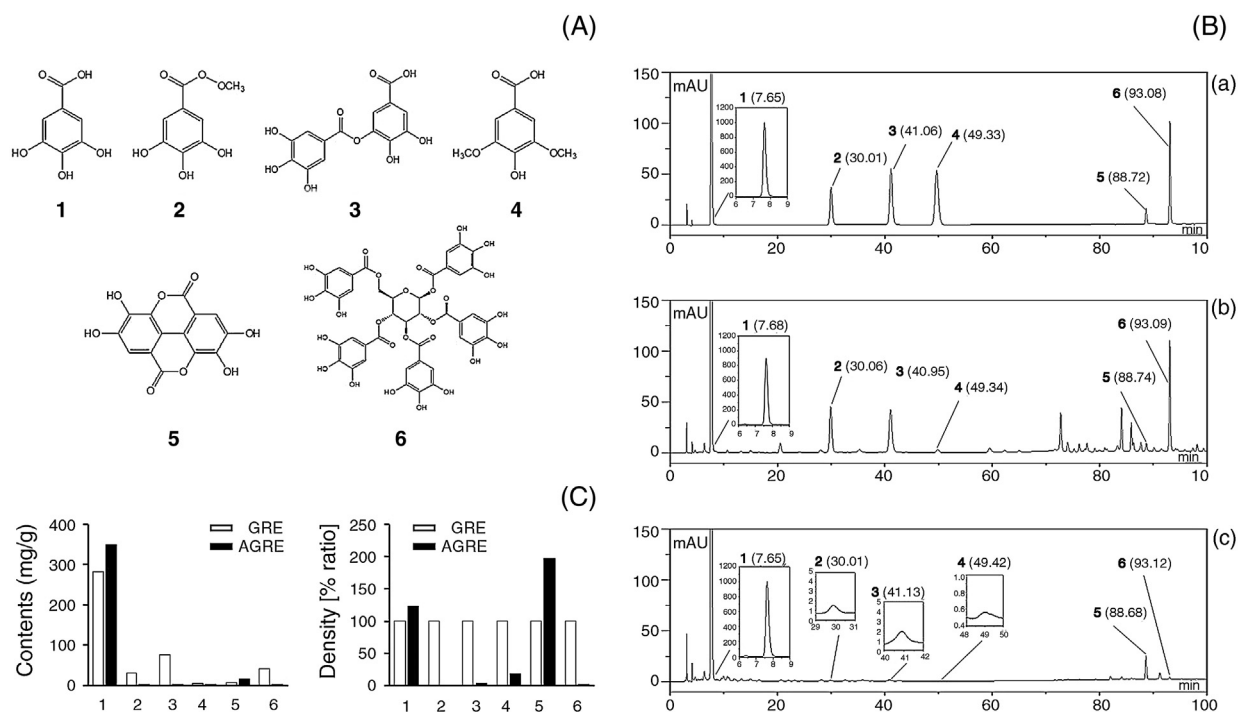


Fig. 1 – HPLC–DAD analysis of six constituents in GRE and AGRE. (A) Chemical structures of six constituents: 1, gallic acid; 2, methyl gallate; 3, digallic acid; 4, syringic acid; 5, ellagic acid; and 6, PGG. (B) HPLC–DAD analyses of the six components in GRE and AGRE at 270 nm: (a) mixed standards, (b) GRE, and (c) AGRE. (C) Contents of six components in GRE and AGRE: 1, gallic acid; 2, methyl gallate; 3, digallic acid; 4, syringic acid; 5, ellagic acid; and 6, PGG.

test was determined by analyzing a mixed standard solution in five replicates during 1 day. Precision was expressed as relative standard deviation (RSD, %); the value of RSD within 3% is generally acceptable. The related equation was as follows: $RSD (\%) = [\text{standard deviation (SD)}/\text{mean measured amount}] \times 100$. The recovery test was conducted to evaluate the accuracy of the method. Recoveries were determined by adding three different concentrations of each standard solution into the GRE or AGRE sample solution (20 mg/mL) in triplicate. Recovery (%) was calculated by the following equation: $\text{recovery (A)} = (\text{found amount} - \text{original amount})/\text{spiked amount} \times 100$.¹⁸

2.2. Cell-based assay

2.2.1. Chemicals and reagents

Dulbecco's modified Eagle's medium was obtained from Lonza (Walkersville, MD, USA). Fetal bovine serum, penicillin, streptomycin, and peroxidase-conjugated secondary antibodies were purchased from Hyclone (Logan, UT, USA). Propidium iodide (PI) and 3-(4,5-dimethylthiazol-2-yl)-2,5-diphenyl-tetrazolium bromide (MTT) were purchased from Sigma Chemical Co. (St. Louis, MO, USA). Caspase-Glo 3/7, caspase-8, and caspase-9 assay kits were purchased from Promega (Madison, WI, USA). For immunoblotting, caspase-3, caspase-8, caspase-9, poly (ADP-ribose) polymerase (PARP), extracellular signal-regulated kinase (ERK), phospho-ERK, p38, phospho-p38, c-Jun NH2-terminal kinase (JNK), phospho-JNK, α -tubulin, and glyceraldehyde 3-phosphate dehydrogenase

(GAPDH) were purchased from Cell Signal Technology, Inc. (Boston, MA, USA).

2.2.2. Cell culture

Various human cancer cell lines, obtained from the Korean Cell Line Bank (Seoul, Korea) and American Type Culture Collection (Rockville, MD, USA), were cultured in Dulbecco's modified Eagle's medium with 10% fetal bovine serum containing 100 units/mL penicillin G and 100 μ g/mL streptomycin. All cells were cultured in an atmosphere of 5% CO₂ at 37 °C.

2.2.3. Cell viability assay

Cells ($3\text{--}5 \times 10^3$ cells/well) were seeded in a 96-well plate and treated with various concentrations of GRE or AGRE for 24 hours. After treatment, cell viability was analyzed by MTT assay as described previously.¹⁹ Color intensity was measured in terms of absorbance at 570 nm with an enzyme-linked immunosorbent assay (ELISA) microplate reader (Sunrise; TECAN, Männedorf, Switzerland).

2.2.4. Cell cycle analysis

Cells were seeded at a density of 1×10^5 cells/mL in a six-well plate and treated with 50 μ g/mL and 100 μ g/mL of GRE or AGRE for 24 hours. The PI staining for cell cycle analysis was performed as described previously.¹⁹ DNA contents of the stained cells were analyzed by FACSCalibur flow cytometry using CellQuest software (Becton-Dickinson, Franklin Lakes, NJ, USA).

Table 1 – Linear regression date, LOD, and LOQ of investigated compounds from Galla Rhois

Analytes	Linear regression data			LOD ^b (μg/mL)	LOQ ^c (μg/mL)
	Linear range (μg/mL)	r ²	Regressive equation ^a		
Gallic acid	0.5–1000	1.0000	y = 186,801x – 145,236	0.05	0.15
Methyl gallate	0.20–100	0.9999	y = 215,623x + 153,590	0.04	0.13
Digallic acid	0.5–100	0.9995	y = 107,350x – 133,444	0.09	0.26
Syringic acid	0.5–100	0.9994	y = 143,259x – 132,447	0.06	0.19
Ellagic acid	0.5–100	1.0000	y = 119,577x – 411,970	0.08	0.23
PGG	0.2–100	0.9997	y = 203,960x – 379,570	0.04	0.13

^a Here, y = peak area (MAU) and x = concentration (μg/mL) of the components.
^b LOD = 3 × signal-to-noise ratio.
^c LOQ = 10 × signal-to-noise ratio.
LOD, limit of detection; LOQ, limit of quantification.

2.2.5. Western blot analysis

The cell lysates treated with GRE or AGRE for Western blot analysis were prepared as described previously.¹⁹ The same amount of protein for each sample was electrophoresed and transferred onto the polyvinylidene difluoride membrane Millipore (Millipore, Billerica, MA, USA). The membranes were incubated at 4 °C overnight with primary antibodies specific for caspase-3, caspase-8, caspase-9, PARP, ERK, phospho-ERK, p38, phospho-p38, JNK, phospho-JNK, α-tubulin, and GAPDH (1:1000), followed by incubation for 1 hour with the corresponding secondary antibody (1:5,000). Specific proteins were detected using a Supersignal West Pico Chemiluminescent Substrate (Pierce, Rockford, IL, USA) and an ImageQuant LAS 4000 mini (GE Healthcare, Piscataway, NJ, USA). Band intensities were calculated using ImageJ software (National Institute of Health, Bethesda, MD, USA).

2.2.6. Statistical analysis

Data were presented as means ± SD. The statistically significant differences between control and botulin-treated cells

were calculated by the Student t test. Values of $p < 0.05$ and $p < 0.01$ were considered to indicate statistical significance.

3. Results

3.1. Validation of quantitative methods

The results of linearity, limit of detection, and limit of quantification analyses for each key analyte are summarized in Table 1. Good linearity of the analytical method was confirmed by correlation coefficients ($r^2 > 0.9994$). Limit of detection and limit of quantification values were in the range of 0.04–0.09 μg/mL and 0.13–0.26 μg/mL, respectively. RSD values for inter- and intraday variation were within the range of 0.51–1.47% and 0.84–2.57%, respectively. The value of RSD was less than 3%, and these results showed an acceptable precision. The recovery ratio of the six standard compounds ranged from 99% to 104% (Table 2). These results indicated that the developed method had reliable accuracy.

Table 2 – Repeatability (n = 3) and recoveries of investigated compounds from Galla Rhois

Peak	Analytes	Spiked amount (μg/mL)	Measured amount (μg/mL)	Recovery (%)	Interday (RSD %)	Intraday (RSD %)
1	Gallic acid	1,402.10	1,402.21 ± 0.20	99	0.87	1.75
		701.05	701.14 ± 0.10	100	1.01	1.89
		350.52	350.32 ± 0.20	100	0.45	0.84
2	Methyl gallate	124.65	124.52 ± 0.20	102	1.42	2.74
		62.32	62.12 ± 0.20	100	1.20	1.97
		31.16	31.04 ± 0.10	104	0.81	2.07
3	Digallic acid	302.55	302.38 ± 0.10	101	0.51	1.42
		151.27	151.27 ± 0.01	99	0.78	1.84
		75.63	75.54 ± 0.20	99	1.11	1.40
4	Syringic acid	18.73	18.53 ± 0.20	100	1.45	2.14
		9.36	9.11 ± 0.20	102	1.34	1.85
		4.68	4.71 ± 0.10	99	1.47	2.57
5	Ellagic acid	27.78	27.75 ± 0.10	100	0.84	1.57
		13.89	13.71 ± 0.20	99	1.42	1.84
		6.95	6.89 ± 0.10	100	0.95	1.01
6	PGG	165.90	165.98 ± 0.05	101	1.41	2.48
		82.95	82.90 ± 0.05	100	1.24	2.21
		41.47	41.35 ± 0.10	101	1.36	1.64

3.2. Change in chemical properties of GRE following the steaming process

In the present study, HPLC was used to analyze the six components present in GRE and AGRE using optimized HPLC–diode array UV/VIS detector chromatographic conditions. The six components, including gallic acid, methyl gallate, digallic acid, syringic acid, ellagic acid, and PGG, were detected at 270 nm based on the stability and higher maximum absorption rates of the major components at baseline (268 nm for gallic acid, 269 nm for methyl gallate, 275 nm for digallic acid, 273 nm for syringic acid, 253 nm for ellagic acid, and 277 nm for PGG; Fig. 1A, 1B). The retention time of gallic acid, methyl gallate, digallic acid, syringic acid, ellagic acid, and PGG were 7.65 minutes, 30.01 minutes, 41.06 minutes, 49.33 minutes, 88.72 minutes, and 93.08 minutes, respectively. In the present study, Contents of the six components in GRE and AGRE were quantified using UV and mass spectroscopy spectra, and their retention times were compared with those of standards using an optimized method. The quantitative analysis data are shown in Fig. 1C. The contents of gallic acid (123.3%) and ellagic acid (196.6%) in AGRE were higher than the contents in GRE (100%). In contrast, methyl gallate (1.4%), digallic acid (4.2%), syringic acid (18.5%), and PGG (2.5%) were less presented in AGRE compared with GRE (100%).

3.3. Inhibition of cell growth by GRE and AGRE in various human cancer cells

To further characterize the inhibitory actions of GRE and AGRE against cancer cells, five different human cancer cell lines [HCT116 (colon), AGS (stomach), MM231 (breast), A549 (lung), and SK-Hep-1 (liver)] were treated with 50 $\mu\text{g/mL}$, 100 $\mu\text{g/mL}$, and 200 $\mu\text{g/mL}$ of GRE or AGRE for 24 hours. The viability of HCT116, A549, and SK-Hep-1 cells was inhibited by over 60% by treatment with 100 $\mu\text{g/mL}$ and 200 $\mu\text{g/mL}$ of GRE or AGRE (Fig. 2A). The viability of HCT116 cells was reduced by about 50% and 64% by treating with 100 $\mu\text{g/mL}$ and 200 $\mu\text{g/mL}$ of GRE, respectively. The viability was reduced by approximately 75% and 80% by AGRE at the same concentrations. Additionally, the growth inhibitory effect of AGRE on HCT116 cells was significantly greater than that of GRE. To further define the inhibitory action of GRE and AGRE on colon cancer cells, the inhibition ratios of each constituent in GRE and AGRE against two colon cancer cell lines, HCT116 and HT29, were evaluated. In HCT116 cells, except digallic acid, the other constituents, including gallic acid, methyl gallate, syringic acid, ellagic acid, and PGG, inhibited cell growth in a dose-dependent manner for 24 hours (Fig. 2B). In contrast, the viability of HT29 cells was affected by about 40% by ellagic acid (from 12.5 μM to 100 μM). Based on these data, the present study focused on HCT116 cells for subsequent tests.

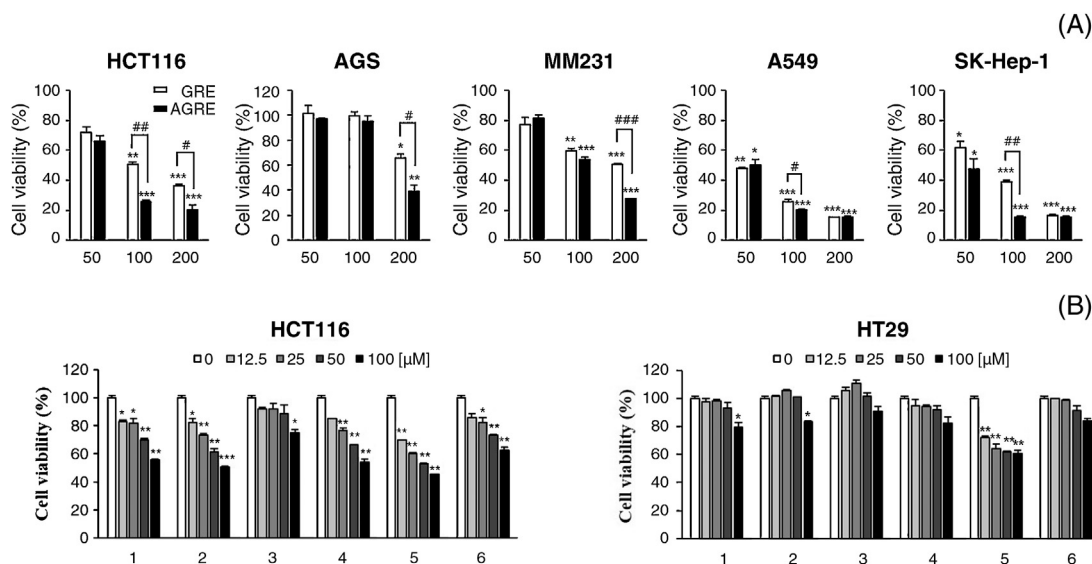


Fig. 2 – Inhibition of cell viability by GRE or AGRE in several human cancer cells. (A) Cells were treated with 50 $\mu\text{g/mL}$, 100 $\mu\text{g/mL}$, and 200 $\mu\text{g/mL}$ of GRE or AGRE for 24 hours. Cell viability was determined by MTT assay, and the results are expressed as the percentages of viable cells compared with those of untreated cells. The data are shown as the means \pm SD of three independent experiments. * $p < 0.05$, ** $p < 0.01$, and *** $p < 0.001$ versus untreated cells. # $p < 0.05$, ## $p < 0.01$, and ### $p < 0.001$ versus GRE-treated cells. * $p < 0.05$, ** $p < 0.01$, and *** $p < 0.001$ versus untreated cells. # $p < 0.05$, ## $p < 0.01$, and ### $p < 0.001$ versus GRE-treated cells. **(B)** Cells were treated with the indicated concentrations of six components in GRE and AGRE for 24 hours in two kinds of human colon cancer cells, HCT116 and HT29. Six components are as follows: 1, gallic acid; 2, methyl gallate; 3, digallic acid; 4, syringic acid; 5, ellagic acid; and 6, PGG. Cell viability was determined by MTT assay and the results are expressed as the percentages of viable cells compared to untreated cells. The data are shown as the means \pm SD of three independent experiments. * $p < 0.05$, ** $p < 0.01$, and *** $p < 0.001$ versus untreated cells. The data are shown as the means \pm SD of three independent experiments.

3.4. Comparison of cell cycle progression in HCT116 cells between GRE and AGRE

After treatment with GRE or AGRE for 24 hours, HCT116 cells were stained with PI, and their cell cycle progression was assessed using flow cytometry. Treatment of cells with 50 $\mu\text{g}/\text{mL}$ and 100 $\mu\text{g}/\text{mL}$ of GRE induced the cell population of sub-G1 phase up to 2.90% and 6.65%, respectively (Fig. 3A). AGRE also induced the cell population of sub-G1 phase to about 5.06% and 11.73% at the same concentrations. In the S phase, 100 $\mu\text{g}/\text{mL}$ of GRE induced the accumulation of 16.22% of cells, which increased about 1.4-fold compared with that in untreated cells (vehicle, 11.44%). Compared with the vehicle, treatment with 100 $\mu\text{g}/\text{mL}$ of AGRE slightly reduced the S-phase cell population in the S phase. However, 100 $\mu\text{g}/\text{mL}$ of AGRE induced a 4.5-fold increase in the sub-G1 cell population, which enhanced the induction of cell death about 1.8-fold compared with that observed with GRE (Fig. 3B).

3.5. Inhibitory effect of GRE and AGRE on HCT116 cell growth

To determine whether the cell death by GRE and AGRE is related to the apoptotic effects in HCT116 cells, the

expression of caspase activities, including activities of caspase-3, caspase-8, and caspase-9, was assessed using Western blot analysis. After 24 hours of treatment with GRE, the caspases were activated and PARP cleavage was observed in HCT116 cells (Fig. 4A). Almost all the caspases were activated by treatment with 100 $\mu\text{g}/\text{mL}$ of GRE. In particular, the expression of caspase-3 and caspase-9 showed increases of about 1.81- and 1.83-fold, respectively, compared with those in untreated cells. In contrast, AGRE showed activation of caspases at 50 $\mu\text{g}/\text{mL}$ concentration for the same duration. AGRE also markedly increased PARP cleavage in a dose-dependent manner. In comparison with GRE, AGRE showed over two-fold increase in the expression of caspase-8, while the expression of caspase-3 or caspase-9 was not affected or weakly upregulated (Fig. 4B).

To identify the antiproliferative effects of GRE and AGRE in HCT116 cells, expressions of cell proliferation-mediated proteins were analyzed by Western blotting. The level of phosphorylated JNK was decreased by about 19% by treating with 100 $\mu\text{g}/\text{mL}$ of GRE, but that of ERK and p38 at the same concentration remained unaffected (Fig. 4C). In contrast, 100 $\mu\text{g}/\text{mL}$ of AGRE inhibited the phosphorylation of ERK and JNK by about 30% and 67%, respectively; notably, the phosphorylation of p38 remained unaffected. Compared with GRE,

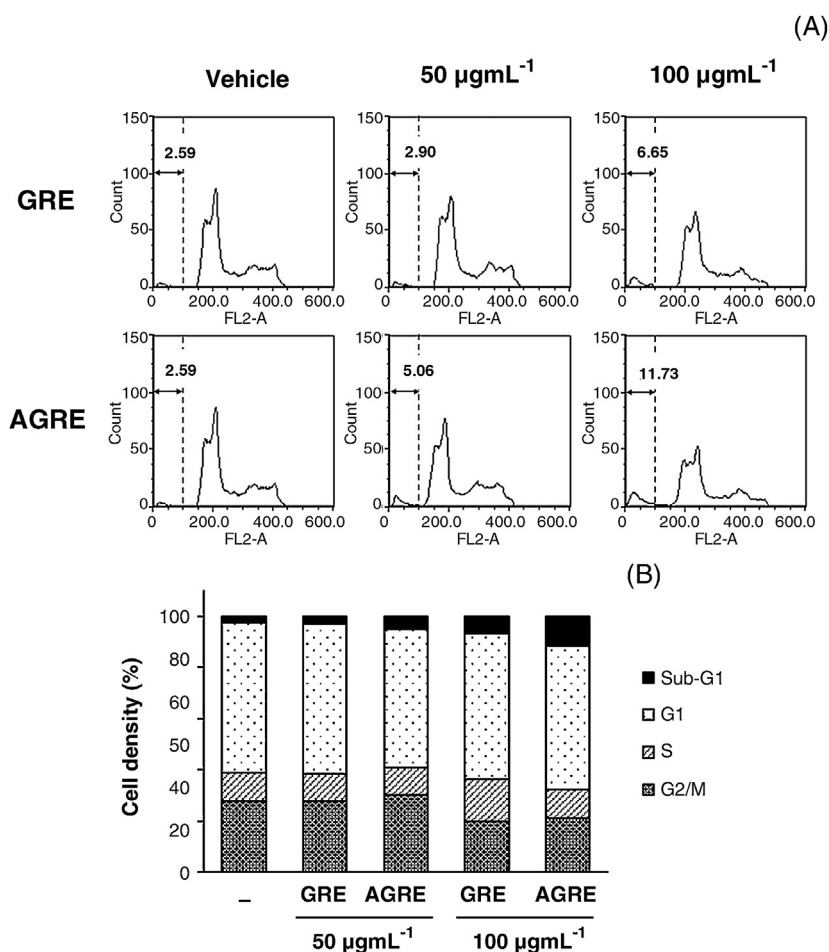


Fig. 3 – Effects of GRE and AGRE on cell cycle progression in HCT116 cells. (A) Cells were treated with 50 $\mu\text{g}/\text{mL}$ and 100 $\mu\text{g}/\text{mL}$ of GRE or AGRE for 24 hours, fixed with prechilled 70% ethanol, stained with propidium iodide solution, and then subjected to flow cytometry for determination of cell cycle distribution. (B) Histogram represents cell cycle analysis on HCT116 cells.

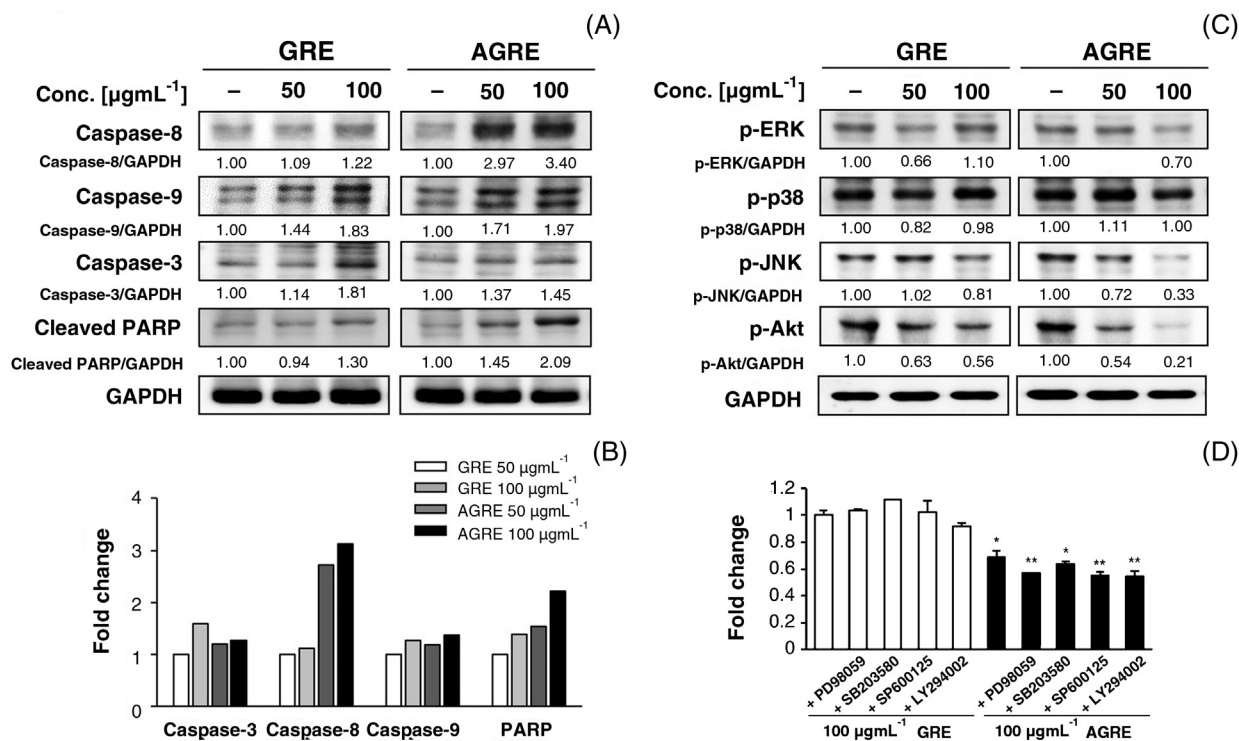


Fig. 4 – Comparison of anticancer effects between GRE and AGRE on protein levels in HCT116 cells. **(A)** Induction of apoptosis by GRE or AGRE in HCT116 cells. The cells were exposed to 50 $\mu\text{g/mL}$ and 100 $\mu\text{g/mL}$ of GRE or AGRE for 24 hours; protein levels were determined by Western blot analyses. The band intensity was calculated and compared with that of untreated cells using ImageJ after normalization relative to GAPDH expression. **(B)** Histogram represents the fold changes of activated caspase-3, caspase-8, and caspase-9 by AGRE compared with that of GRE. **(C)** Antiproliferative effects of GRE and AGRE on HCT116 cells. The cells were exposed to 50 $\mu\text{g/mL}$ and 100 $\mu\text{g/mL}$ of GRE or AGRE for 24 hours, and then subjected to Western blot analyses to determine the levels of phosphorylated forms of MAPK proteins, including ERK, p38, and JNK (or AKT). **(D)** Investigation of the antiproliferative effects of GRE and AGRE for 24 hours using the MAPK cascade inhibitors PD98059 (10 μM), SB203580 (5 μM), and SP600125 (10 μM), and the PI3K inhibitor LY294002 (10 μM). Cell viability was determined by MTT assay. The results show the means \pm SD of three independent experiments. * $p < 0.05$ and ** $p < 0.01$ versus GRE treated cells.

AGRE (100 $\mu\text{g/mL}$) suppressed the phosphorylation of JNK by approximately two-fold. At 50 $\mu\text{g/mL}$ concentrations, GRE and AGRE strongly inhibited AKT phosphorylation by over 40%. Furthermore, at 100 $\mu\text{g/mL}$ concentrations, AGRE suppressed the phosphorylation of AKT by approximately two-fold more than that of GRE. To confirm the antiproliferation effects of GRE and AGRE on A549 cells, the cells were pre-treated with specific inhibitors, such as PD98059 (ERK1/2 inhibitor), SB203580 (p38 inhibitor), SP600125 (JNK inhibitor), and LY294002 for 1 hour, followed by treatment with 100 $\mu\text{g/mL}$ of GRE and AGRE for 24 hours. The antiproliferation effect of GRE was increased in LY294002 by about 9%, whereas it did not increase in the other inhibitors such as PD98059, SB203580, and SP600125. Under the same conditions, pretreatment with inhibitors, such as PD98059, SP600125, and LY294002, followed by AGRE treatment markedly enhanced cell death. SP600125 and LY294002 improved the antiproliferation effect of AGRE up to 19% and 20%, respectively, whereas SB203580 weakly improved the antiproliferation effect by about 7% (Fig. 4D).

4. Discussion

GR has resulted in the characterization of gallotannins, which have been considered to possess medicinal properties and numerous benefits.^{20,21} Among the constituents of GR, gallotannins are a type of hydrolyzable tannin consisting of a central glucose core, surrounded by several gallic acid units attached by depside bonding of additional galloyl residues.^{22,23} Furthermore, GR is rich in well-known phenolic acids, such as gallic acid and methyl gallate that account for nearly 20% and 7%, respectively.^{10,24} Based on these preliminary reports, we investigated the changes in the constituents and biological activities of GRE when physical heat was applied using the steaming process at high temperature and pressure with an autoclaved system. In the processing of specific herbal medications, steaming treatment has been applied to enhance the desirable effects and reduce the side effects by changing the chemical constituents. Steaming of ginseng at 120°C produced ginsenosides F₄, Rg₃, and Rg₅, not present in raw ginseng, and they were evaluated for their

anticancer effects.^{25,26} Through the steaming process, rhubarb showed an increase in monoanthrone compounds such as anthraquinones and a decrease in dianthrone compounds such as sennosides, which enhanced its antimicrobial and anti-inflammatory effects.² Furthermore, heat-treated licorice increased the total polyphenol content, which is involved in antioxidant activity.³ Here, the processing of GRE generated a different chemical profile compared with the nonprocessed GRE. The components that structurally changed following the processing include gallic acid, ellagic acid, and PGG. Several *in vitro* and *in vivo* studies have shown that gallic acid, a typical phenolic acid, possesses antioxidant and radical scavenging activities that are involved in exerting anticancer effects.²⁷ Ellagic acid is a hydrolyzable tannin constituted polymers of gallic acid, linked to glucose centers to form the class of compounds known as ellagitannins.²⁸ It also possesses potent anticarcinogenic/antimutagenic properties against a variety of carcinogens, including nitrosamines, azoxymethane, and mycotoxins, and a strong antioxidant activity.^{29,30} In previous reports, it has been demonstrated that ellagic acid protects hepatocytes from damage by reactive oxygen species.³⁰ In addition, it has been reported that ellagic acid exerts potent preventive and therapeutic effects against several types of cancers, including colon, breast, prostate, skin, and esophageal cancers, and osteogenic sarcoma.³¹ It selectively induces reactive oxygen species-mediated apoptosis in cancerous B lymphocytes of patients with chronic lymphocytic leukemia.²⁸ The present results demonstrated that gallic acid and ellagic acid were markedly increased in AGRE compared with GRE. These constituents strongly induced cell death in human colon cancer cells, suggesting that AGRE may show an increased radical scavenging effect, and these effects may affect cell death, which may enhance apoptosis in HCT116 cells. Notably, *in vitro* studies have shown that GRE containing PGG inhibits tumor growth through the suppression of angiogenesis and metastasis of cancer cells.^{32,33} In AGRE, the contents of PGG were significantly reduced by processing, which may also be involved in the increase of galloyl residues such as gallic acid and ellagic acid. The characteristic anticancer effect of PGG, for instance, antiangiogenic or antimetastatic activity, was not identified in GRE and AGRE. Therefore, further studies are necessary to establish whether AGRE enhances the anticancer effect of GRE against angiogenesis and metastasis.

Based on these preliminary observations, molecular mechanisms underlying the anticarcinogenic effects of AGRE were assessed in HCT cells. Using Western blot analyses, AGRE was shown to influence the expression levels of caspase-8, caspase-9, and caspase-3. The caspase cascades are divided into two major pathways: an extrinsic pathway containing caspase-8 and caspase-10, which is initiated by the ligand-mediated activation of cell surface death receptors, and an intrinsic pathway containing caspase-9, which is activated by intracellular signals from the mitochondria.^{34,35} In the present study, compared with GRE, AGRE markedly activated caspase-8 and caspase-9, although the activation of caspase-3 was weakly induced. This suggests that AGRE led to strong apoptosis via a caspase-dependent pathway, which may enhance the anticancer effect of GRE in HCT116 cells.

MAPKs regulate cellular processes such as proliferation, differentiation, and apoptosis of cells.³⁶ In particular, pharmacological modulation of MAPK signals influences the apoptotic response to antitumor agents.³⁷ The present results demonstrated that AGRE inhibits the activation of ERK and JNK, while p38 remained unaffected. GRE did not affect the signals of MAPK cascades, including ERK, JNK, and p38, involved in inducing apoptosis in HCT116 cells. Additionally, the inhibition of MAPK signaling by treatment of specific protein inhibitors (ERK inhibitor PD98059, p38 inhibitor SB203580, and JNK inhibitor SP600125) improved the cell death of AGRE, whereas these inhibitors did not contribute to the apoptotic function of GRE in HCT116 cells. Phosphorylation of AKT, a cell survival-related protein, was strongly inhibited by both GRE and AGRE, which confirmed that the inhibition of AKT improves cell death in HCT116 by GRE and AGRE using treatment with LY294002. Therefore, we suggest that the antiproliferative activity of AGRE results from suppressing the MAPK and AKT signaling pathways, whereas that of GRE results from inhibiting AKT activation only.

We elucidated the enhancement of anticancer effect of AGRE by steaming processing of GRE using the analysis of chemical profiling and molecular mechanism study in human colon cancer cells HCT116. The enhanced apoptotic effect of AGRE was presumed to be attributed to the changes in the pattern of gallotannins in GRE. In the case of molecular signals associated with cell proliferation, AGRE showed different signals compared with GRE, which demonstrated a strong antiproliferation effect in HCT116 cells. These results would support the fact that the steaming process may be a feasible method for improving the anticancer effects of GRE.

Conflicts of interest

All authors have no conflicts of interest to declare.

Acknowledgments

This work was supported by a grant (K16281) awarded to the Korean Institute of Oriental Medicine by the Ministry of Education, Science and Technology (MEST), Korea.

REFERENCES

1. Kim JS, Kim HJ, Ma JY, Kim JM. Studies on the processing of herbal medicines (II)-HPLC analysis of standard compounds of unprocessed and processed herbal medicines. *Korean J Pharmacogn* 2002;33:305-7 [In Korean, English abstract].
2. Doui M, Kakiuchi N, Mikage M. Chemical differences between steamed rhubarbs with or without pre-processing with liquor. *J Trad Med* 2010;27:109-14.
3. Lee JR, Jo MJ, Park SM, Kim SC, Park SJ. Establishment of UPLC method for analysis of liquiritigenin and studies on the processing of licorice for enhancement of liquiritigenin content. *Korean J Orient Med Prescrip* 2010;18:145-54 [In Korean, English abstract].
4. Shin YW, Kim DH, Kim NJ. Studies on the processing of crude drugs (VII)—on the constituents and biological

- activities of Gardeniae Fructus by processing. *Korean J Pharmacogn* 2003;34:45–54 [In Korean, English abstract].
5. Kim HK, Kim YA, Hwang SW, Ko BS. Quantitative analysis of 6-gingerol in the Zingiberis Rhizoma by processing methods. *Korean J Pharmacogn* 2002;33:291–5 [In Korean, English abstract].
 6. Kim JS, Kim HJ, Ko JH. Studies on the processing of herbal medicines (III)—HPLC analysis of magnonol and inhibitory effects on the formation of advanced glycation endproducts (AGEs) of unprocessed-and processed magnolia bark. *Korean J Pharmacogn* 2002;33:308–11 [In Korean, English abstract].
 7. Kitagawa I, Fukuda Y, Taniyama T, Yoshikawa M. Chemical studies on crude drug processing. VII. On the constituents of Rehmanniae Radix. (1): absolute stereostructures of rehmaglutins A, B, and D isolated from Chinese Rehmanniae Radix, the dried root of *Rehmannia glutinosa* LIBOSCH. *Chem Pharm Bull* 1991;39:1171–6.
 8. Zhu YP. *Chinese materia medica*. Amsterdam: Harwood Academic Publishers; 1998:659–60.
 9. Duke JA, Ayensu ES. *Medicinal plants of China*. Algonac, MI: Reference Publications, Inc.; 1985.
 10. Djakpo O, Yao W. *Rhus chinensis* and *Galla Chinensis*—folklore to modern evidence: review. *Phytother Res* 2010;24:1739–47.
 11. Kee CH, Walter MW. *The pharmacology of Chinese herbs*. 2nd ed. Boca Raton, FL: CRC Press LLC; 1999.
 12. Xiao CH, Yang SS, Hong XK. *Chemistry of traditional Chinese medicine*. Shanghai: Science and Technology Publishing House; 2000.
 13. Zhang J, Li L, Kim SH, Hagerman AE, Lu J. Anti-cancer, anti-diabetic and other pharmacologic and biological activities of penta-galloyl-glucose. *Pharm Res* 2009;26:2066–80.
 14. Lee HJ, Seo NJ, Jeong SJ, Park Y, Jung DB, Koh W, et al. Oral administration of penta-O-galloyl-beta-D-glucose suppresses triple-negative breast cancer xenograft growth and metastasis in strong association with JAK1-STAT3 inhibition. *Carcinogenesis* 2011;32:804–11.
 15. Yin S, Dong Y, Li J, Lu J, Hu H. Penta-1,2,3,4,6-O-galloyl-beta-D-glucose induces senescence-like terminal S-phase arrest in human hepatoma and breast cancer cells. *Mol Carcinog* 2011;50:592–600.
 16. Lee JJ, Cho WK, Kwon H, Gu M, Ma JY. *Galla rhois* exerts its antiplatelet effect by suppressing ERK1/2 and PLCbeta phosphorylation. *Food Chem Toxicol* 2014;69:94–101.
 17. Han Z, Liu X, Ren Y, Luan L, Wu Y. A rapid method with ultra-high-performance liquid chromatography–tandem mass spectrometry for simultaneous determination of five type B trichothecenes in traditional Chinese medicines. *J Sep Sci* 2010;33:1923–32.
 18. He D, Shan Y, Wu Y, Liu G, Chen B, Yao S. Simultaneous determination of flavanones, hydroxycinnamic acids and alkaloids in citrus fruits by HPLC–DAD–ESI/MS. *Food Chem* 2011;127:880–5.
 19. Yim NH, Cho WK, Lee JH, Jung YP, Yang HJ, Ma JY. HRT, herbal formula, induces G2/M cell cycle arrest and apoptosis via suppressing Akt signaling pathway in human colon cancer cells. *Evid Based Complement Alternat Med* 2012;2012:871893.
 20. Feldman KS, Sahasrabudhe K, Smith RS, Scheuchenzuber WJ. Immunostimulation by plant polyphenols: a relationship between tumor necrosis factor-alpha production and tannin structure. *Bioorg Med Chem Lett* 1999;9:985–90.
 21. Tian F, Li B, Ji B, Yang J, Zhang G, Chen Y, et al. Antioxidant and antimicrobial activities of consecutive extracts from *Galla chinensis*: the polarity affects the bioactivities. *Food Chem* 2009;113:173–9.
 22. Xiang P, Lin Y, Lin P, Xiang C, Yang ZW, Lu ZM. Effect of cationization reagents on the matrix-assisted laser desorption/ionization time-of-flight mass spectrum of Chinese gallotannins. *J Appl Polym Sci* 2007;105:859–64.
 23. Tian F, Li B, Ji B, Zhang G, Luo Y. Identification and structure–activity relationship of gallotannins separated from *Galla chinensis*. *LWT Food Sci Technol* 2009;42:1289–95.
 24. Buziashvili IS, Kommissarenko NF, Kovalev IP, Gordienko VG, Kolesnikov DG. The structure of gallotannins. *Chem Nat Comp* 1973;9:752–5.
 25. Kim WY, Kim JM, Han SB, Lee SK, Kim ND, Park MK, et al. Steaming of ginseng at high temperature enhances biological activity. *J Nat Prod* 2000;63:1702–4.
 26. Kim YC, Hong HD, Rho J, Cho CW, Rhee YK, Yim JH. Changes of phenolic acid contents and radical scavenging activities of ginseng according to steaming times. *J Ginseng Res* 2007;31:230–6.
 27. Bhimani RS, Troll W, Grunberger D, Frenkel K. Inhibition of oxidative stress in HeLa cells by chemopreventive agents. *Cancer Res* 1993;53:4528–33.
 28. Salimi A, Roudkenar MH, Sadeghi L, Mohseni A, Seydi E, Pirahmadi N, et al. Ellagic acid, a polyphenolic compound, selectively induces ROS-mediated apoptosis in cancerous B-lymphocytes of CLL patients by directly targeting mitochondria. *Redox Biol* 2015;6:461–71.
 29. Huetz P, Mavaddat N, Mavri J. Reaction between ellagic acid and an ultimate carcinogen. *J Chem Inf Model* 2005;45:1564–70.
 30. Hwang JM, Cho JS, Kim TH, Lee YI. Ellagic acid protects hepatocytes from damage by inhibiting mitochondrial production of reactive oxygen species. *Biomed Pharmacother* 2010;64:264–70.
 31. Zhang HM, Zhao L, Li H, Xu H, Chen WW, Tao L. Research progress on the anticarcinogenic actions and mechanisms of ellagic acid. *Cancer Biol Med* 2014;11:92–100.
 32. Huh JE, Lee EO, Kim MS, Kang KS, Kim CH, Cha BC, et al. Penta-O-galloyl-beta-D-glucose suppresses tumor growth via inhibition of angiogenesis and stimulation of apoptosis: roles of cyclooxygenase-2 and mitogen-activated protein kinase pathways. *Carcinogenesis* 2005;26:1436–45.
 33. Ho LL, Chen WJ, Lin-Shiau SY, Lin JK. Penta-O-galloyl-beta-D-glucose inhibits the invasion of mouse melanoma by suppressing metalloproteinase-9 through down-regulation of activator protein-1. *Eur J Pharmacol* 2002;453:149–58.
 34. Saraste A, Pulkki K. Morphologic and biochemical hallmarks of apoptosis. *Cardiovasc Res* 2000;45:528–37.
 35. Sheikh MS, Huang Y. Death receptors as targets of cancer therapeutics. *Curr Cancer Drug Targets* 2004;4:97–104.
 36. Murphy LO, Blenis J. MAPK signal specificity: the right place at the right time. *Trends Biochem Sci* 2006;31:268–75.
 37. Fan M, Chambers TC. Role of mitogen-activated protein kinases in the response of tumor cells to chemotherapy. *Drug Resist Updat* 2001;4:253–67.